nature neuroscience

Activation of adult-born neurons facilitates learning and memory

Mariana Alonso[1,2], Gabriel Lepousez[1,2], Sebastien Wagner[1,2,4], Cedric Bardy[1–4], Marie-Madeleine Gabellec[1,2], Nicolas Torquet[1,2] & Pierre-Marie Lledo[1,2]

Thousand of local interneurons reach the olfactory bulb of adult rodents every day, but the functional effect of this process remains elusive. By selectively expressing channelrhodopsin in postnatal-born mouse neurons, we found that their activation accelerated difficult odor discrimination learning and improved memory. This amelioration was seen when photoactivation occurred simultaneously with odor presentation, but not when odor delivery lagged by 500 ms. In addition, learning was facilitated when light flashes were delivered at 40 Hz, but not at 10 Hz. Both *in vitro* and *in vivo* electrophysiological recordings of mitral cells revealed that 40-Hz stimuli produced enhanced GABAergic inhibition compared with 10-Hz stimulation. Facilitation of learning occurred specifically when photoactivated neurons were generated during adulthood. Taken together, our results demonstrate an immediate causal relationship between the activity of adult-born neurons and the function of the olfactory bulb circuit.

In rodents, the process of adult neurogenesis produces thousands of new neurons in the adult olfactory bulb every day. It is still debated what functions these new neurons have on the bulb. Recent studies have begun to delineate a role for adult-born neurons in odorant detection[1], perceptual learning[2], short-term[1,3] and long-term[4,5] olfactory memory, odorant discrimination[6–9], innate olfactory responses including predator avoidance and sexual behaviors[10], and olfactory fear conditioning[11]. However, the immediate effect of adult-born neuron activity on a specific olfactory function *in vivo* has not yet been explored.

Inhibitory interneurons contribute to several circuit functions in the olfactory bulb that shape odor discrimination and learning. First, interneurons mediate inhibitory interactions between relay neurons (that is, mitral and tufted cells, hereafter referred to as mitral cells), which support both recurrent and lateral inhibition[12–14]. Second, interneurons receive extensive feedback projections from cortical regions, resulting in feedforward inhibition onto mitral cells[15–17]. It has been demonstrated that local synaptic inhibition is essential for reaching correct odor-discrimination performance[18,19] and for olfactory perceptual learning[2]. Presumably, much of this inhibition arises from granule cells, the most numerous GABAergic interneuron subtype in the olfactory bulb circuit[15].

Granule cells might facilitate odor-discrimination performance by causing mitral cell firing patterns to diverge from similar and confusing sensory inputs resulting from overlapping combinatorial codes of sensory receptor neurons[20]. Because the vast majority of newly formed neurons that reach the olfactory bulb become granule cells[21], we asked whether the activity of these neurons can specifically participate in odor discrimination learning. To do this, we specifically activated early postnatal- and adult-born granule cells during a go/no-go operant conditioning task. We found that activating adult-born neurons, but not early postnatal-born neurons, resulted in a beneficial effect on odor discrimination learning and olfactory memory. This improvement depends on synchronization with odor stimuli and the amount of GABAergic synaptic inhibition that sculpts mitral cell population firing activity *in vivo*.

RESULTS

In vivo light delivery triggers adult-born neuron activity

We used channelrhodopsin-2 (ChR2) to control neuronal activity exclusively in newly formed cells[22]. We injected a lentiviral vector encoding ChR2-YFP (yellow fluorescent protein) under the control of the synapsin 1 (*Syn1*) promoter into the rostral migratory stream (RMS) of mice, resulting in a cohort of light-sensitive new interneurons encompassing granule cells and periglomerular cells (**Fig. 1a**). We did not detect any viral diffusion from the injection site directly to the bulb. The small fraction of ChR2-positive cells expressing doublecortin, a marker of immature newborn neurons (3% at 12 weeks post-injection, wpi), confirmed the absence of a substantial tail to the proliferation of cells expressing ChR2 after viral injection[22]. We restricted our study to mature postnatal-born interneurons (either formed at early postnatal ages or throughout life) by starting experiments at 12 wpi, when the density of newborn granule cells reached a plateau (**Supplementary Fig. 1a**). When performing *ex vivo* patch-clamp recordings, we found that brief flashes of light evoked inward currents in voltage clamp (**Fig. 1b**), and action potentials in current clamp (**Fig. 1b**).

To stimulate light-sensitive neurons *in vivo*, we implanted all of the mice with a miniature LED (465 nm) over the dorsal bulb (**Fig. 1c**).

[1]Institut Pasteur, Laboratory for Perception and Memory, Paris, France. [2]Centre National de la Recherche Scientifique, Unité de Recherche Associée 2182, Paris, France. [3]Present address: The Salk Institute for Biological Studies, Laboratory of Genetics, La Jolla, California, USA. [4]These authors contributed equally to this work. Correspondence should be addressed to P.-M.L. (pmlledo@pasteur.fr).

Received 10 January; accepted 16 April; published online 13 May 2012; doi:10.1038/nn.3108

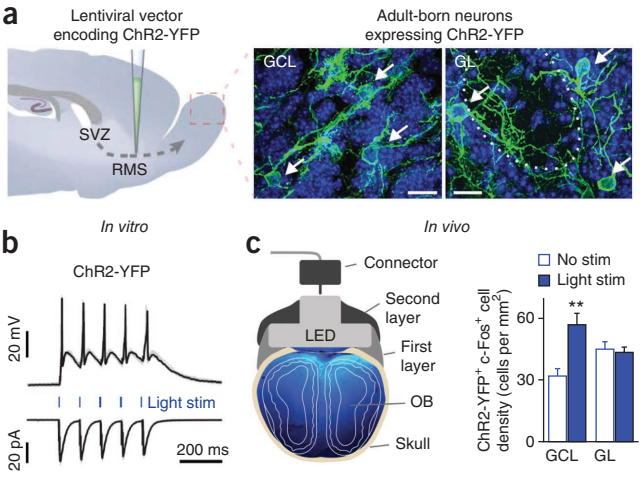

Figure 1 Light-induced activation of adult-born neurons. (**a**) Left, lentiviral vectors encoding ChR2-YFP were injected in the RMS. Right, confocal images of an olfactory bulb (OB) slice showing the immunoreactivity of ChR2-YFP–positive neurons (green) and DAPI staining (blue). Arrows point to YFP-positive cell somas observed in the GCL (middle) and the glomerular layer (GL, right). Scale bars represent 15 µm. The white dashed line delineates a glomerular structure. SVZ, subventricular zone. (**b**) Patch-clamp recordings of an adult-born granule cell expressing ChR2-YFP (10 wpi). Brief flashes of light (5 ms) evoked inward currents at –70 mV (bottom). Action potentials were triggered by light flashes (8 mW mm^{-2}; current clamp = –2 pA, V_m = –68 mV; top). (**c**) Left, schematic of the *in vivo* photostimulation design. The blue/black shading illustrates the penetration depth of the light (see **Supplementary Fig. 2** for quantification). Right, density of YFP and c-Fos double-positive neurons in non-stimulated mice (no stim) and after photostimulation (three 90-s pulse trains at 40 Hz delivered every 2 min, light stim). A significant difference was found between groups only in the GCL (**$P < 0.01$ with a Bonferroni test after repeated measures two-way ANOVA, group $P = 0.04$; 13,226 cells, $n = 4$). Error bars represent s.e.m.

Notably, light activation of ChR2-positive neurons at 40 Hz led to higher expression levels of the immediate early gene *c-Fos* in the granule cell layer (GCL), but not in the glomerular layer (**Fig. 1c** and **Supplementary Fig. 1b–g**). The c-Fos–reactive cell population represented approximately 6.4 ± 0.6% ($n = 4$) of the overall population of YFP-labeled adult-born granule cells. The c-Fos–positive new cells were scattered in the superficial and deep regions of the GCL, suggesting homogeneous activation of granule cells throughout the entire layer, as seen directly by measuring light propagation (**Supplementary Fig. 2**). Taken together, these data confirm and extend previous findings showing that the firing activity of adult-born neurons can be remotely controlled by brief light stimuli[22].

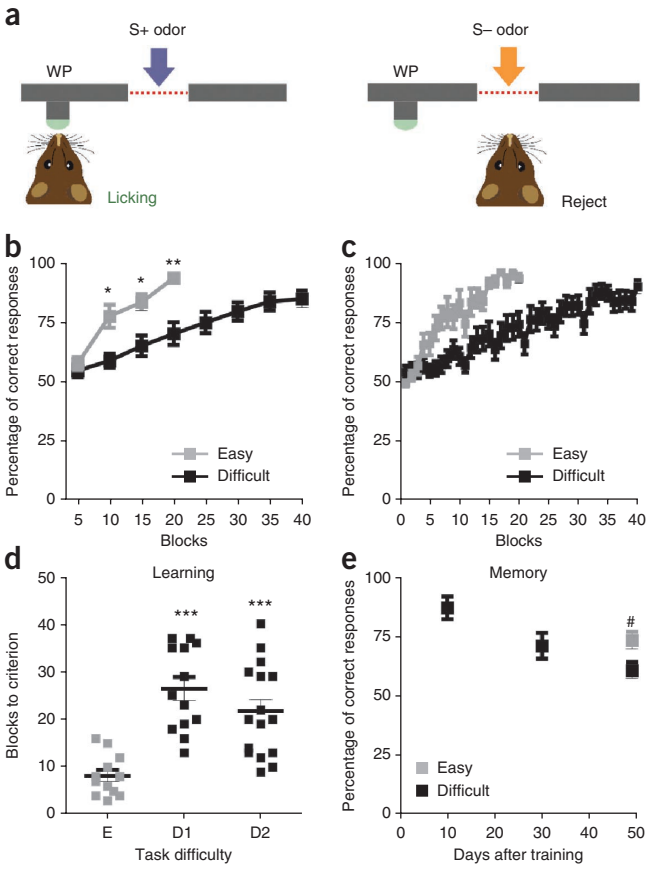

Activation of adult-born neurons facilitates learning

We investigated the potential contribution of adult-born neurons in olfactory learning with a go/no-go operant task in which mice were trained to discriminate easy and difficult odor pairs (**Fig. 2a**). The length of training it takes to discriminate the pair correctly defines the categorization of easy and difficult pairs. Although 85% of correct responses were reached in all cases, control mice needed more training to reach this level when exposed to a difficult pair (**Fig. 2b**,**c**). Similarly, mice required fewer training blocks to reach the criterion number of correct responses when exposed to easy rather than difficult odorant pairs (**Fig. 2d**). No difference was apparent between easy and difficult odor pairs in discrimination time (**Supplementary Fig. 3a**,**b**) or in movement time (**Supplementary Fig. 3c**). Memory was then tested at different post-training days in independent groups of mice (**Fig. 2e**). The initial memory clearly declined at 30 d, although

Figure 2 Olfactory discrimination learning. (**a**) In our task, the mouse breaks a light beam (red dashed line) across the odor port, which initiates a trial. Licking in the water port (WP) in response to a positive odor stimulus (S+) triggers water delivery (that is, the go response, left). In response to a negative odor stimulus (S–), the trained mouse retracts its head (that is, the no-go response, right) and rejects licking. (**b**) Accuracy (mean percentage of correct responses for five training blocks) is shown for easy odor pair (gray squares) and difficult odor pair (black squares). The learning curves of difficult and easy tasks were significantly different (group: $F_{1,28} = 7.2$, $P = 0.01$, repeated measures two-way ANOVA followed by Fisher LSD *post hoc* test, *$P < 0.05$, **$P < 0.01$, $n = 12$–16). A score of 50% corresponds to the success rate at chance level. (**c**) Data are presented as in **b** for the percentage of correct responses for each training block (group $F_{1,23} = 8.57$, $P = 0.007$ with a repeated measures two-way ANOVA, $n = 12$–16). For odor pairs we used 1% anisole versus 1% cineole (E1) and 0.1% (+)-limonene versus 0.1% (–)-limonene (D2). (**d**) Mean number of blocks required to reach the criterion of 85% of correct responses. ***$P < 0.001$, indicates significant differences from an easy task (main effect: $F_{2,38} = 16.61$, $P < 0.0001$, one-way ANOVA followed by Bonferroni *post hoc* test, $n = 12$–16). For odor pairs, we used E1, D2 and 1% (+)-carvone versus 1% (–)-carvone (D1). We defined an easy pair of monomolecular odorants when mice learnt to recognize distinct molecules in less than 200 trials (that is, mean of ten blocks to reach the criterion in control mice), whereas a difficult pair of odorants were molecularly similar odors or mixtures that required at least 360 trials (mean of 18 blocks) to reach the criterion of correct responses. (**e**) Mean percentage of correct responses for the memory test 10, 30 and 50 d post-training in a difficult task. The initial memory was still above chance level at 50 d post-training for both tasks ($P < 0.001$, one sample *t* test versus theoretical mean of 50%, $n = 10$), and was significantly higher for an easy task (E1) than for a difficult one (D2). #$P = 0.012$ with paired Student's *t* test, $n = 10$. Error bars represent s.e.m.

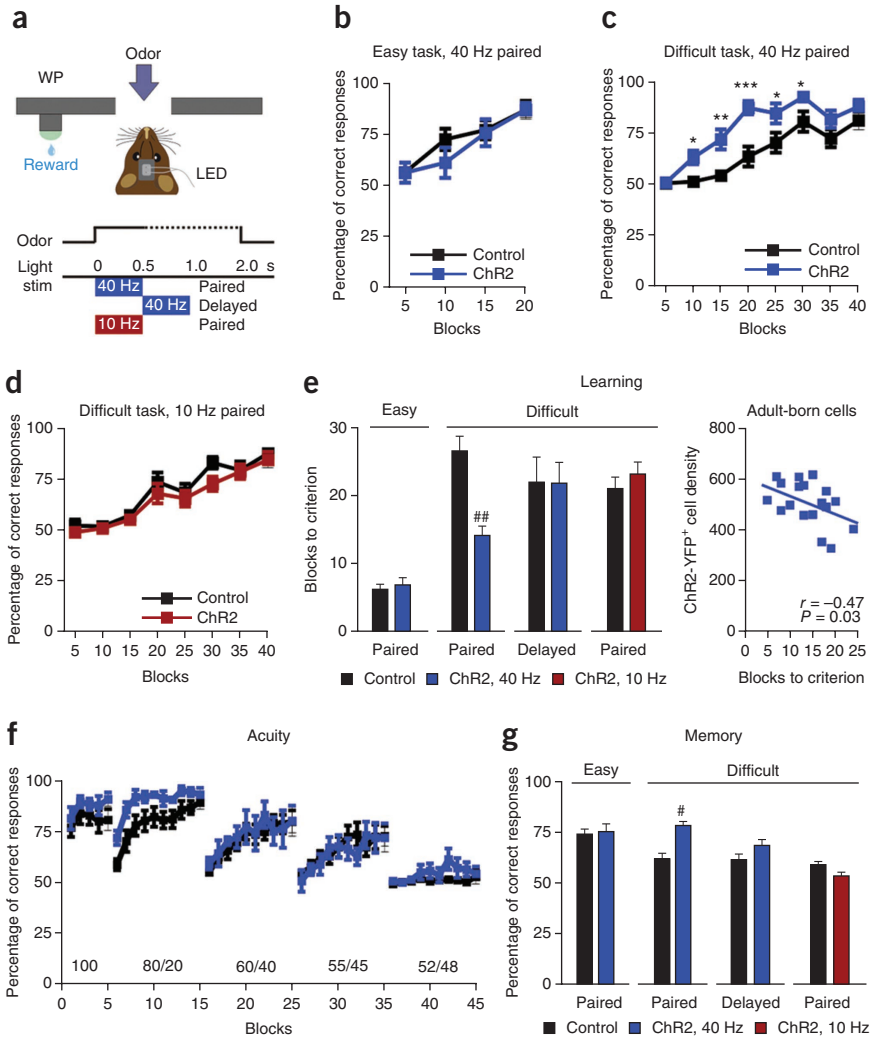

Figure 3 Stimulation of adult-born neurons accelerates learning. (**a**) Diagram of the timing of the task events. Photoactivation (5-ms pulses) was provided at 10 or 40 Hz during a stimulation period of 500 ms, occurring at odor delivery (paired) or 500 ms later (delayed). (**b**,**c**) Paired stimulation of adult-born neurons at 40 Hz did not change the learning rate of an easy task (group $F_{1,18} = 0.26$, $P = 0.61$, repeated measures two-way ANOVA, $n = 8$–13, **b**), whereas a difficult task was learned quicker (group $F_{1,17} = 8.75$, $P = 0.0008$, repeated measures two-way ANOVA, **c**; $^{***}P < 0.001$, $^{**}P < 0.01$, $^{*}P < 0.05$, Fisher LSD test, $n = 8$–13) (see **Supplementary Video 1**). For odor pairs, we used E1 (**b**) and D1 (**c**). (**d**) No effect was found when using 10-Hz light stimulation (group $F_{1,14} = 4.25$, $P = 0.06$ with a repeated measures two-way ANOVA, $n = 8$–10). We used 0.6% of butanol + 0.4% pentanol versus 0.4% of butanol + 0.6% pentanol (D4) as the odor pair. (**e**) Similar results were found when counting the number of blocks required to reach the criterion (left, $^{\#\#}P = 0.003$, Mann-Whitney test, $n = 8$–13), and an inverse correlation was found between the density of ChR2-positive cells (cells per mm^2) counted in the GCL and the number of blocks required to reach the criterion when delivering 40-Hz paired-light stimuli (right, Pearson's test, $n = 19$). For odor pairs, we used D1, 1% (+)-terpinene versus 1% (–)-terpinene (D3), and 0.6% of ethyl-butyrate + 0.4% amyl-acetate versus 0.4% of ethyl-butyrate + 0.6% amyl-acetate (D5). (**f**) To evaluate discrimination acuity, we trained mice to discriminate mixtures with increasing complexity. Mice were first trained to distinguish between 1% (+)-carvone and 1% (–)-carvone. Once mice reached criterion, they were asked to discriminate between mixtures of the same odors. Each day, the ratio of (+)-carvone and (–)-carvone changed in both positive stimulus and negative stimulus odor solution (odor pair D1). The percentage of (+)-carvone/(–)-carvone in the positive stimulus is indicated. Only the last five training blocks are shown for the initial training using pure odors (indicated as 100). Both groups showed identical performance (group effect $F_{1,13} = 0.47$, $P = 0.47$, repeated measures two-way ANOVA, $n = 8$–13). (**g**) To assess memory, we tested mice 50 d after the discrimination task. The photostimulation (10 or 40 Hz) was applied simultaneously with odor onset (paired using E1 and D1 for 40 Hz and D4 for 10 Hz), or 500 ms after (delayed using D2), at both training and test sessions. $^{\#}P = 0.015$, significant differences between control and ChR2 groups with a Mann-Whitney test ($n = 7$–13). Error bars represent s.e.m.

performance was still above chance level at 50 d. Notably, the 50-d memory test was significantly higher for an easy task than for a difficult one ($P = 0.012$; **Fig. 2e**).

We then used this operant conditioning task to test whether the specific activation of adult-born neurons could affect learning (**Fig. 3**). Mice injected with lentiviral vectors (ChR2 group) and control mice (control group) were first trained on an easy task while receiving light stimulation (40 Hz) beginning at the odor onset and lasting for 500 ms (**Fig. 3a**). This duration was set to match the mean discrimination time measured for this task (**Supplementary Fig. 3b**). Previous *in vivo* findings indicate that, following odor stimulation, activated granule cells typically fire up to ~40 Hz[23] and receive spontaneous high-frequency barrages of excitatory postsynaptic potentials at 35 Hz[24]. Light activation of newly formed neurons did not modify the learning rate of an easy task (**Fig. 3b**). In contrast, odor-paired stimulation at 40 Hz markedly accelerated the acquisition of a difficult discrimination (**Fig. 3c** and **Supplementary Fig. 4a**). Although all of the mice learned the task to criterion, mice spent less effort to learn the discrimination when ChR2-positive adult-born neurons were activated at 40 Hz, as reflected in the number of blocks required to reach criterion (**Fig. 3e**). Notably, we found an inverse correlation between the number of light-sensitive new cells and the minimum blocks to criterion (**Fig. 3e**). Light stimulation had two requirements to be effective: the light needed to be delivered at high rather than low frequencies (40 Hz versus 10 Hz; **Fig. 3c**,**d**), and light activation had to occur simultaneously with the odorant, as no improvement was seen when light was delivered 500 ms after the odor onset (**Fig. 3a**,**e** and **Supplementary Fig. 4b**), corresponding to the movement time in this task (**Supplementary Fig. 3c**). In control experiments without light stimulation, we observed no differences in performance, which allowed us to discard potential off-target effects of viral vector expression (**Supplementary Fig. 4c**). Moreover, light stimulation produced no difference in learning performance in either easy or difficult tasks in control mice, indicating that light has no nonspecific effects on task performance (**Supplementary Fig. 4d**–**f**).

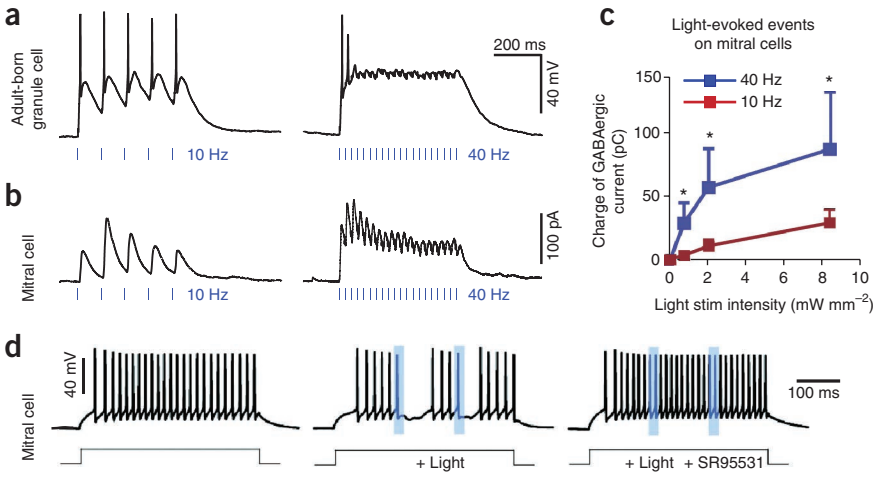

Figure 4 Light-induced responses in granule and mitral cells *in vitro*. (**a**) Patch-clamp recordings of an adult-born granule cell at 10 wpi. Brief flashes of light (5 ms, ≥2 mW mm^{-2}, V_m = –68 mV) delivered at 10 or 40 Hz depolarized the membrane potential and triggered action potentials. (**b**) Patch-clamp recordings of a mitral cell recorded in olfactory bulb slices at 10 wpi. Brief flashes of light (5 ms, 8.4 mW mm^{-2}) were delivered at 10 and 40 Hz (voltage clamp = 0 mV). (**c**) A plot of the charge of light-induced synaptic GABAergic current in response to different light intensities and frequencies. The total charge of currents evoked at 40 Hz was significantly higher than those evoked by 10 Hz (*P < 0.05 with a Wilcoxon paired test, n = 10). Charge of GABAergic current is expressed in pico-Coulombs. (**d**) Traces of current-clamp recordings showing the firing activity of a mitral cell, which was depolarized above spike threshold by injecting a steady-step current (+100 pA, V_m = –62 mV). Mitral cell firing was repeatedly inhibited by blue light activation of adult-born neurons. The specific $GABA_A$R antagonist SR95531 totally blocked the light-evoked synaptic inhibition (n = 12). Error bars represent s.d.

To determine whether activation of adult-born neurons can further improve odor discrimination acuity, we trained mice to discriminate mixtures with increasing difficulty. Mice were first trained in a difficult task while receiving light stimuli (40 Hz; **Fig. 3c**). We then carried out a morphing experiment by mixing the odors in both positive stimulus and negative stimulus solutions (**Fig. 3f**). A different mixture ratio was tested each day. Both groups showed similar maximal performance in all of the mixtures tested, indicating that activation of adult-born neurons did not improve odor discrimination acuity. The same result was found in another difficult task based on a mixture with which mean maximal performance did not exceed 75% (**Supplementary Fig. 5a**,**b**). The discrimination time between different tasks and protocols remained unchanged (**Supplementary Fig. 5c**), supporting the notion that odor investigation did not vary with the degree of the task difficulty (**Supplementary Fig. 3b**), and no differences were found in detection threshold and motivation (**Supplementary Fig. 5d**,**e**).

We next analyzed whether light activation of newly formed cells also altered olfactory memory. Mice were tested for odor memory recall 50 d after the end of the training session. Once again, memory improvement was found in the ChR2 group only when a paired protocol (40 Hz) was used during the learning of difficult odorant pairs (**Fig. 3g**). This effect was specific to memory because the two groups had indistinguishable performance in the initial and final training sessions (**Supplementary Fig. 6a**,**b**).

Light-induced responses in granule and mitral cells

To explore the cellular and synaptic events mediated by the selective activation of ChR2-positive adult-born interneurons in the olfactory bulb network, we first characterized light-induced responses using patch-clamp recordings from slices. Whole-cell recordings from visually identified ChR2-positive adult-born granule cells (8–12 wpi; **Fig. 4a**) revealed reliable firing in response to light stimuli delivered at 10 Hz (5-ms light pulses; **Fig. 4a**). Notably, a significant decrease of light-evoked spike fidelity was observed with a 40-Hz stimuli (firing rate: 10-Hz stimuli, 10.5 ± 1.4 Hz; 40-Hz stimuli, 3.5 ± 0.6 Hz; Wilcoxon paired test, P = 0.017, n = 7; **Fig. 4a**). To characterize the consequences of 10- and 40-Hz light stimulation protocols on postsynaptic GABAergic inhibition, we performed whole-cell recordings of mitral cell in slices containing ChR2-positive adult-born interneurons. Mitral cells are the principal output neurons of the olfactory bulb and constitute the main postsynaptic target of adult-born neurons[22]. Both 10- and 40-Hz stimuli resulted in reliable inhibitory postsynaptic currents that follow the temporal pattern imposed by the 10- and 40-Hz light protocols with high fidelity (**Fig. 4b**). With both trains of stimuli, inhibitory postsynaptic currents depressed and stabilized, as classically described using electrical stimulation[25,26]. Thus, despite reduced spike fidelity in single neurons, 40-Hz stimulation of adult-born neurons triggered precise and reliable inhibition of postsynaptic mitral cells at the population level. Notably, the net charge of inhibitory currents evoked by the 40-Hz train stimuli was always significantly higher than that evoked with 10 Hz (P = 0.0098 for 0.8 mW mm^{-2}, P = 0.002 for 2.1 mW mm^{-2} and P = 0.002 for 8.3 mW mm^{-2}; **Fig. 4c**). We next asked whether light-evoked inhibitory synaptic events recorded in mitral cells could modulate their firing activity *in vitro*. Mitral cell firing activity evoked by short depolarizing current steps (that is, 600–800-ms duration) delivered above the spiking threshold was reliably inhibited by short light pulses (25 ms; **Fig. 4d**). This inhibition was blocked by bath application of a competitive $GABA_A$ receptor antagonist (10 µM SR95531; **Fig. 4d**), indicating that photoactivation of adult-born interneurons inhibits mitral cell firing via activation of $GABA_A$ receptors.

We next investigated *in vivo* how the olfactory bulb responded to the light stimulation delivered at the frequencies that we used during behavioral experiments. We performed extracellular recordings in awake head-restrained mice (n = 5) of mitral cell firing activity coupled to local light delivery in the GCL nearby the recorded cells. Taking into account the density of ChR2-positive granule cells and the characteristics of the optic fiber, we estimated that the cone of light stimulated approximately 1,100–1,400 cells (see Online Methods). Recordings performed at 16 wpi from randomly selected well-identified single units showed spontaneous mitral cell firing activity at ~22 Hz (**Fig. 5a**,**b**) with some bursts of activity time-locked to the respiratory rhythm (data not shown, but see ref. 27). Local light stimulation strongly suppressed spontaneous firing during a short time window (**Fig. 5c**), supporting the notion that the population of ChR2-positive adult-born granule cells can be reliably controlled by a brief pulse of light in the awake mouse. Light-evoked firing suppression

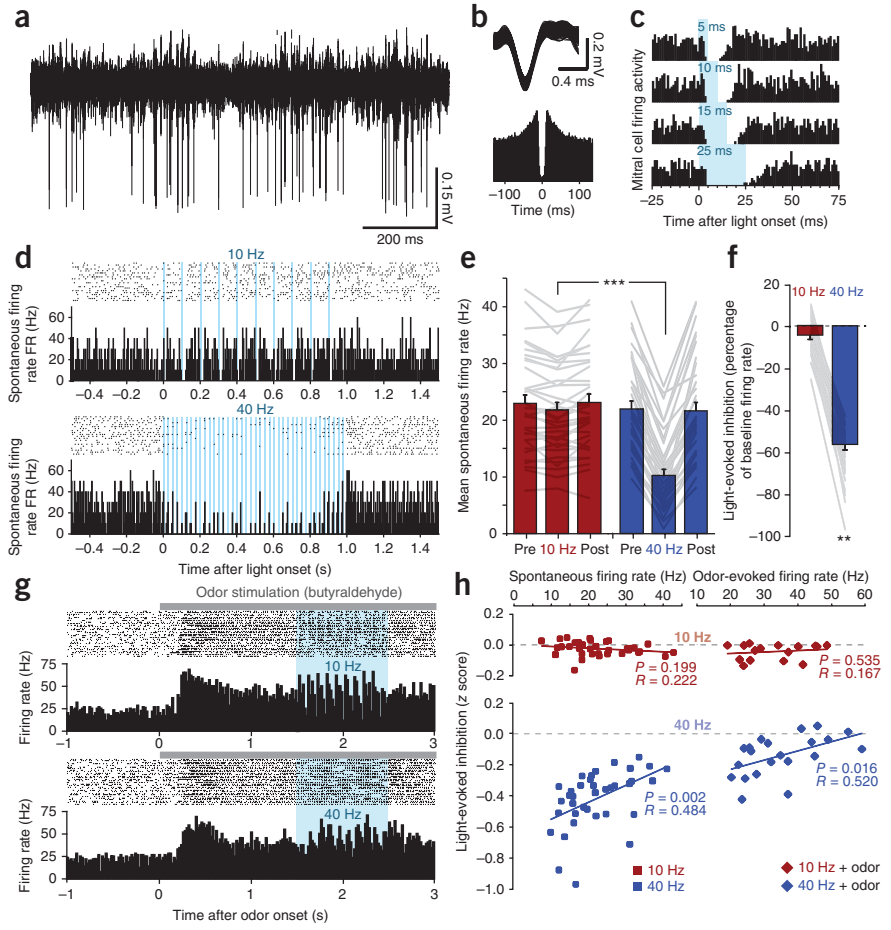

Figure 5 Light-activation of ChR2-positive adult-born neurons control spontaneous and odor-evoked mitral cell firing activity in the awake mouse. (**a**) Example recording of spontaneous spiking activity of a mitral cell in the olfactory bulb of an awake head-restrained mouse. (**b**) Confirmation of single-cell recording by the similar spike waveform and amplitude ($n = 500$ spikes, top) and spike train autocorrelogram showing a clear refractory period (bottom). (**c**) Example peristimulus time histogram (PSTH) of mitral cell spontaneous spiking activity showing clear light-evoked inhibition after local stimulation (5, 10, 15 and 25 ms) through an optical fiber aimed at the neighboring GCL of the recorded cell. (**d**) PSTH and raster plots (20 sweeps) of mitral cell spontaneous spiking activity after 10-Hz (5 ms, 10 pulses, top) and 40-Hz light stimulation (5 ms, 40 pulses, bottom). (**e**) Mean spontaneous mitral cell firing rate 1 s before (pre), during 1-s light stimulation at 10 Hz (red, $n = 35$) or 40 Hz (blue, $n = 37$), and 1 s after (post). Gray lines show results from individual cells. $^{***}P < 10^{-9}$, *t* test. (**f**) Histograms summarizing the percentage change of spontaneous firing inhibited by light after 10-Hz (red) and 40-Hz (blue) stimulation. Gray lines show data from individual cells recorded for both light stimuli ($n = 35$, $^{**}P < 10^{-18}$, paired *t* test). (**g**) PSTH and raster plots (30 sweeps) showing the influence of 10-Hz (5 ms, 10 pulses, top) and 40-Hz (5 ms, 40 pulses, bottom) light stimulation on odor-evoked mitral cell activity (odor stimulation, 3 s; odor valve opening at $t = 0$). (**h**) Magnitude of light-evoked inhibition of mitral cell spontaneous (square, left) and odor-evoked (diamond, right) firing activity during 10-Hz (red, spontaneous firing, $n = 35$ cells; odor evoked, $n = 16$ cells) and 40-Hz (blue, spontaneous firing, $n = 37$ cells; odor evoked, $n = 21$ cells) stimulation as a function of individual mean firing activity (Pearson's correlation coefficient *R* and *P* values are indicated). Error bars represent s.e.m.

increased with light-pulse duration (5–25 ms; **Fig. 5c**) and was absent in mice lacking ChR2 expression (data not shown). Notably, all of the recorded mitral cells exhibited substantial light-evoked inhibition of firing (paired t test for each cell, light stimulation versus pre-stimulation, $P < 0.05$, $n = 37$ of 37), supporting previous findings that nearly all mitral cells are targeted by adult-born neurons[22].

We next evaluated the effect of 10- and 40-Hz train stimuli on mitral cell firing activity. Although spontaneous firing was briefly suppressed after each light impulse, the mean spontaneous firing rate of mitral cells was barely altered by the 10-Hz train stimuli ($-4.4 \pm 1.4\%$, $n = 35$, paired *t* test, $P < 0.0001$; **Fig. 5d–f**). In contrast, mitral cell firing activity was markedly reduced by the 40-Hz stimuli ($-55.8 \pm 2.7\%$, $n = 37$, paired *t* test, $P < 10^{-12}$; **Fig. 5d–f**), confirming the greater efficiency of the 40-Hz protocol in triggering synaptic GABA release (**Fig. 4c**) and inhibiting mitral cell spontaneous firing activity (**Fig. 5e,f**). At 10-Hz stimulation, increasing light-pulse duration from 5 to 25 ms only weakly increased light-evoked inhibition (percentage change in firing rate after 10-Hz stimulation with 10-ms pulse duration, $-3.9 \pm 2.1\%$, $P = 0.12$; 15-ms pulse duration, $-5.3 \pm 5.1\%$, $P = 0.09$; 25-ms pulse duration, $-8.4 \pm 5.1\%$, $P = 0.07$, $n = 10$, paired *t* test), confirming the specific effect on firing suppression of the frequency rather than the overall light duration.

In addition to this selective effect, we investigated how light stimuli delivered to adult-born neurons might regulate odor-induced firing of mitral cells, focusing on the excitatory responses of mitral cells to odors (mean odor-evoked increase in firing rate $+88.5 \pm 8.0\%$). Odor presentation and stimulation (10 or 40 Hz) during the steady-state phase of the odorant-induced response increased mitral cell firing activity (**Fig. 5g**). In contrast with spontaneous firing, 10- or 40-Hz stimulation did not change the mean odor-evoked firing rate. To better characterize this differential effect between spontaneous and odor-evoked activity, we analyzed the relationship between the magnitude of inhibition triggered by 10- and 40-Hz train stimuli and the mean firing rate of individual cells (**Fig. 5h**). A strong correlation was exclusively observed at 40 Hz, but not at 10 Hz, for both spontaneous ($n = 35$–37 cells; **Fig. 5h**) and odor-evoked firing activity ($n = 16$–21 cells; **Fig. 5h**). As a result, when mitral cell spiking was high, 40-Hz light–induced inhibition was less efficient at suppressing firing (**Fig. 5h**). During odor presentation, the 40-Hz light stimulation reformatted the input-output relationship of excitatory responses in favor of highly active mitral cells (**Fig. 5h**). Taken together, these data suggest that 40-Hz stimulation of adult-born interneurons suppresses firing in weakly activated mitral cells and favors the response of highly active neurons in the overall mitral cell population.

Early postnatal-born neurons differ from adult-born neurons

To determine whether learning and memory could be enhanced specifically by activating adult-born neurons, lentiviral vectors were injected into postnatal day 6 (P6) pups. The volume of the injected

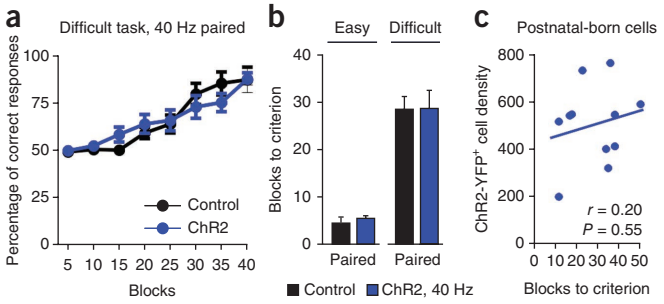

Figure 6 Light stimulation of postnatal-born neurons does not modify odor discrimination learning. (**a**) Paired stimulation at 40 Hz of postnatal-born neurons did not change the learning rate of an easy and a difficult task (group $F_{1,16} = 0.0007$, $P = 0.97$ with repeated measures two-way ANOVA, $n = 7–11$). (**b**) Similar results were found when counting the number of blocks required to reach the criterion ($P > 0.05$, Mann-Whitney test, $n = 7–11$). (**c**) No correlation was found between the density of postnatal-born ChR2-positive cells (cells mm^{-2}) counted in the GCL and the number of blocks required to reach criterion when delivering 40-Hz paired light stimuli (Pearson's test, $n = 11$). For odor pairs, we used E1 and D4. Error bars represent s.e.m.

vectors was adjusted to reach a similar density of transduced cells between postnatal and adult bulb circuits at 12 wpi (**Supplementary Fig. 7a**). With early postnatal-born granule cells expressing ChR2, light stimuli did not improve the learning rate, regardless of the difficulty of the task (**Fig. 6a**,**b** and **Supplementary Fig. 7b**), and no correlation was found between the number of postnatal-born neurons and animal performance (**Fig. 6c**). In addition, the discrimination time between different groups remained unchanged (**Supplementary Fig. 7c**). Collectively, these results point to the specific behavioral effect of recruiting new granule cells generated throughout adult life, but not during early postnatal development.

DISCUSSION

Our results demonstrate a direct functional effect of adult-born interneuron activity on both odor learning and memory. Activation of adult-born neurons facilitates discrimination learning only when the task is difficult. This refinement is specific for neurons born during adulthood and depends on light frequency and synchronization with odorant stimuli. We found a correlation between the number of adult-born neurons that were sensitive to light and animal performance, which further suggests that the inhibition mediated by adult-born neurons facilitates associative learning. Finally, *in vivo* recordings revealed that 40-Hz light activation of adult-born neurons inhibited both spontaneous and odor-evoked mitral cell firing activity in weakly activated mitral cells and favored the response of highly active neurons.

Previous studies have reported interactions between adult neurogenesis and fine odor discrimination[2,6,9,28], olfactory memory[1,3–5] and fear conditioning[11]. However, other reports have concluded that adult neurogenesis is dispensable for learned responses to chemical cues[29], but is essential for innate olfactory responses[10]. These apparent discrepancies might result from the use of different learning procedures and/or behavioral tasks based on varying difficulty[21]. In general, previous studies used approaches that were not completely selective (for example, concomitant partial ablation of hippocampal neurogenesis) and/or induce a long-term ablation of adult neurogenesis, which may recruit progressive homeostatic mechanisms and thereby contribute to the discrepancies. In this context, our study is, to the best of our knowledge, the first to show an immediate causal relationship between adult neurogenesis and circuit function.

When two odor stimuli are dissimilar, the excitatory path from the olfactory epithelium through the bulb to the olfactory cortex seems sufficiently resolved for odor discrimination in both mammals and insects, resulting in fast learning (**Supplementary Fig. 8a**). However, when the olfactory system receives similar inputs (a difficult discrimination), these signals may be confused by overlapping information in the spatial (for example, ref. 30) and temporal dimensions (for example, ref. 31) (**Supplementary Fig. 8b**). As a consequence, during a difficult discrimination task, mice[18,19] and insects[32,33] require extensive active learning, likely triggering plasticity in the olfactory bulb network, to disentangle these ambiguous sensory inputs[34]. Part of this cellular/network plasticity could be mediated by the massive top-down inputs to the olfactory bulb circuit[15–17,35,36] and/or downstream targets[37]. We found that light-induced inhibition mediated by adult-born neurons, but not by early postnatal-born neurons, accelerated difficult learning (**Supplementary Fig. 8c**). Adult-born cells might participate in the learning-dependent plasticity required to disambiguate the patterns of bulb network activity during difficult learning. Notably, light stimulation improved learning, but not acuity, supporting the idea that the learning process itself was improved. It is important to stress that difficult tasks took longer, but mice nevertheless reached a stable performance exceeding 85% of correct responses. As a result, our procedure is not fully appropriate for detecting differences in maximal performance[19]. In contrast, when a two-alternative choice procedure is used, rats and mice performed with lower accuracy on more difficult task[38,39]. In this context, the use of a different procedure will be required to completely unravel the contribution of adult-born neurons to both learning and discrimination accuracy. An alternative method of determining the role of adult-born cells to learning and memory would be loss-of-function experiments using halorhodopsin to specifically inhibit these cells.

How does granule cell activation facilitate difficult learning? Granule cell–mediated inhibition onto mitral cells is essential for early processing of olfactory information[19,20,32] and is a locus of experience-dependent plasticity[40,41]. One possibility is that light-induced inhibition mimics feedforward inhibition supplied by top-down fibers impinging onto new granule cells[15–17]. Alternatively, the combination of repetitive activation of granule cell–to–mitral cell synapses and light-evoked activation might provide an experience-dependent increase in inhibitory transmission during a training session (**Supplementary Fig. 8c**). As mitral cell inhibition reaches a threshold, feedforward inhibition may sharpen the distinction between neural representations of similar odorants and thereby facilitate odorant discrimination during a learning process (**Supplementary Fig. 8c**). Consistent with this hypothesis, our *in vitro* and *in vivo* electrophysiological results indicate that stimulation at 40 Hz produces greater net inhibition of mitral cells than when they are given at 10 Hz. The 40-Hz stimuli may produce sufficient inhibition to push the olfactory bulb network across the threshold at which information disambiguation begins to occur. In addition, our *in vivo* results show that highly activated mitral cells resist light-evoked inhibition after odor presentation, suggesting that activation of adult-born granule cells can also enhance the contrast between mitral cells with regard to differences in their firing rate. This observation suggests that one potential mechanism responsible for improved learning may involve the ability of adult-born granule cells to dynamically control the gain of mitral cells in favor of highly activated cells (**Fig. 5h**). Alternatively, the reformatting of mitral cell output might be interpreted as a form of noise reduction. With a preferential redistribution of population activity toward strongly activated cells, light-evoked activation of adult-born granule cells might reduce correlated noise

in the mitral cell population and thereby improve downstream integration of olfactory information to achieve stable and meaningful olfactory representations[42]. Further experiments will be required to determine whether the inhibition promoted by light stimulation might reinforce the synchronization of odor-activated neighbor mitral cells, which may also contribute to a better integration of olfactory information by the olfactory cortex[43].

Our results support a view in which olfactory behaviors that are sensitive to the recruitment of adult-born neurons are those in need of inputs from higher brain centers and/or synaptic plasticity between granule cells and mitral cells. Previous results showing that the selective survival of new granule cells depends on learning[5,7,8,44] support this observation. In addition, it is known that, during odorant learning, contextual and top-down processes change mitral cell responses to odor stimuli[35,36,45].

Is enhanced odor learning a consequence of improved selective attention? Learning facilitation depends on light-stimulation frequency and synchronization with odorant stimuli. Given that light-evoked activation of newborn cells improved odor discrimination learning (**Fig. 3c**), but not discrimination acuity (**Fig. 3f**), olfactory attention may not be directly modulated by activation of newborn cells. Thus, it is unlikely that our findings are a result of an extra-activity of granule cells that can attract the mouse's attention only during learning phase. Nevertheless, we cannot rule out that granule cell activity (particularly adult-born granule cell activity) is involved in some attentional processes. Further experiments will be required to evaluate the role of attention and other state-dependent regulations on odor discrimination learning.

Animals trained with paired-light stimuli had stronger memory than controls. This is consistent with results obtained from irradiated mice in which impaired adult neurogenesis was associated with deficient long-term memory[4] and results showing that immature neurons are recruited by long-term odor memory recall[5]. However, it is still unknown whether the improvement of odor memory that we observed is just a consequence of enhancing odor discrimination learning or if it is a result of the direct action of adult-born neurons on memory consolidation and/or memory retrieval.

We found that about 6% of the overall population of labeled new granule cells responded to light stimuli as assessed by c-Fos staining, a method that likely underestimates the number of light-activated cells. How can a small fraction of activated newly formed granule cells be capable of inducing major behavioral changes? Computational modeling has shown that small and restricted changes in granule cell activation lead to widespread changes in inhibitory inputs onto mitral cells[46,47]. This is further supported by our *in vitro* and *in vivo* findings, which suggest that most principal neurons are functionally connected with adult-born granule cells. The highly divergent action from a few granule cells to several mitral cells might be crucial for adult-born neurons to adjust bulbar odorant representation that is necessary for discrimination and memory. In contrast with our selective stimulation of newborn granule cells, the specific reduction of inhibitory strength from the entire population of granule cells altered early odor processing, but not olfactory learning and memory[19]. Together, these results indicate that pre-existing and adult-generated granule cells have distinct functions in processing olfactory inputs. Finally, our results also suggest that early-postnatal and adult-generated granule cells have distinct functions in processing olfactory inputs. Further investigation will be needed to clarify what is unique about the inhibition provided by adult-born neurons and, in particular, if this allows them to enhance pattern separation in the olfactory bulb circuit[48]. This unique action of adult-born neurons could originate from their intrinsic electrophysiological (passive and active) membrane properties, their unique synaptic contacts[40] or their distinct cellular targets[22]. Together, our results suggest that adult-born granule cell–mediated inhibition is important during olfactory discrimination learning and memory. These findings indicate that the olfactory bulb does not merely relay sensory information from the olfactory epithelium to the olfactory cortex, but instead actively participates in olfactory learning and memory, two processes that take advantage of the continuous arrival of adult-born bulbar neurons.

METHODS

Methods and any associated references are available in the online version of the paper.

Note: Supplementary information is available in the online version of the paper.

ACKNOWLEDGMENTS

We thank G. Gheusi for his advice regarding the use of olfactometers, L. Petreanu for the manipulation of the LEDs during behavioral experiments, K. Murray and N. Maffey for technical assistance, and M. Valley and G. Gheusi for their critical reading of the manuscript. We thank the ENP Network for Viral Transfer for viral vector production. This work was supported by NovalisTaitbout, the Letten Foundation, the Foundation pour la Recherche Medical, the Agence Nationale de la Recherche (ANR-BLAN-SVSE4-LS-110624 and ANR-09-NEUR-004 in the frame of "ERA-NET NEURON" of FP7 program by the European Commission).

AUTHOR CONTRIBUTIONS

M.A. and P.-M.L. designed the experiments, discussed the results and wrote the manuscript. M.A. performed surgery, behavioral experiments and analyzed data. G.L. designed, performed and analyzed *in vivo* electrophysiology recordings. S.W. design olfactomers and light-stimulation devices. C.B. performed and analyzed *in vitro* electrophysiology recordings. M.-M.G. performed immunohistochemistry and N.T. designed the database for behavioral analysis.

COMPETING FINANCIAL INTERESTS

The authors declare no competing financial interests.

Published online at http://www.nature.com/doifinder/10.1038/nn.3108.
Reprints and permissions information is available online at http://www.nature.com/reprints/index.html.

1. Breton-Provencher, V., Lemasson, M., Peralta, M.R. & Saghatelyan, A. Interneurons produced in adulthood are required for the normal functioning of the olfactory bulb network and for the execution of selected olfactory behaviors. *J. Neurosci.* **29**, 15245–15257 (2009).
2. Moreno, M.M. *et al.* Olfactory perceptual learning requires adult neurogenesis. *Proc. Natl. Acad. Sci. USA* **106**, 17980–17985 (2009).
3. Rochefort, C., Gheusi, G., Vincent, J.D. & Lledo, P.M. Enriched odor exposure increases the number of newborn neurons in the adult olfactory bulb and improves odor memory. *J. Neurosci.* **22**, 2679–2689 (2002).
4. Lazarini, F. *et al.* Cellular and behavioral effects of cranial irradiation of the subventricular zone in adult mice. *PLoS ONE* **4**, e7017 (2009).
5. Sultan, S. *et al.* Learning-dependent neurogenesis in the olfactory bulb determines long-term olfactory memory. *FASEB J.* **24**, 2355–2363 (2010).
6. Enwere, E. *et al.* Aging results in reduced epidermal growth factor receptor signaling, diminished olfactory neurogenesis, and deficits in fine olfactory discrimination. *J. Neurosci.* **24**, 8354–8365 (2004).
7. Mandairon, N. *et al.* Neurogenic correlates of an olfactory discrimination task in the adult olfactory bulb. *Eur. J. Neurosci.* **24**, 3578–3588 (2006).
8. Alonso, M. *et al.* Olfactory discrimination learning increases the survival of adult-born neurons in the olfactory bulb. *J. Neurosci.* **26**, 10508–10513 (2006).
9. Mouret, A., Lepousez, G., Gras, J., Gabellec, M.M. & Lledo, P.M. Turnover of newborn olfactory bulb neurons optimizes olfaction. *J. Neurosci.* **29**, 12302–12314 (2009).
10. Sakamoto, M. *et al.* Continuous neurogenesis in the adult forebrain is required for innate olfactory responses. *Proc. Natl. Acad. Sci. USA* **108**, 8479–8484 (2011).
11. Valley, M.T., Mullen, T.R., Schultz, L.C., Sagdullaev, B.T. & Firestein, S. Ablation of mouse adult neurogenesis alters olfactory bulb structure and olfactory fear conditioning. *Front. Neurosci.* **3**, 51 (2009).
12. Yokoi, M., Mori, K. & Nakanishi, S. Refinement of odor molecule tuning by dendrodendritic synaptic inhibition in the olfactory bulb. *Proc. Natl. Acad. Sci. USA* **92**, 3371–3375 (1995).
13. Lledo, P.M. & Lagier, S. Adjusting neurophysiological computations in the adult olfactory bulb. *Semin. Cell Dev. Biol.* **17**, 443–453 (2006).

14. Cleland, T.A. Early transformations in odor representation. *Trends Neurosci.* **33**, 130–139 (2010).
15. Shepherd, G.M., Chen, W.R., Willhite, D., Migliore, M. & Greer, C.A. The olfactory granule cell: from classical enigma to central role in olfactory processing. *Brain Res. Rev.* **55**, 373–382 (2007).
16. Matsutani, S. & Yamamoto, N. Centrifugal innervation of the mammalian olfactory bulb. *Anat. Sci. Int.* **83**, 218–227 (2008).
17. Mouret, A., Murray, K. & Lledo, P.M. Centrifugal drive onto local inhibitory interneurons of the olfactory bulb. *Ann. NY Acad. Sci.* **1170**, 239–254 (2009).
18. Abraham, N.M. *et al.* Maintaining accuracy at the expense of speed: stimulus similarity defines odor discrimination time in mice. *Neuron* **44**, 865–876 (2004).
19. Abraham, N.M. *et al.* Synaptic inhibition in the olfactory bulb accelerates odor discrimination in mice. *Neuron* **65**, 399–411 (2010).
20. Murthy, V.N. Olfactory maps in the brain. *Annu. Rev. Neurosci.* **34**, 233–258 (2011).
21. Lazarini, F. & Lledo, P.M. Is adult neurogenesis essential for olfaction? *Trends Neurosci.* **34**, 20–30 (2011).
22. Bardy, C., Alonso, M., Bouthour, W. & Lledo, P.M. How, when, and where new inhibitory neurons release neurotransmitters in the adult olfactory bulb. *J. Neurosci.* **30**, 17023–17034 (2010).
23. Tan, J., Savigner, A., Ma, M. & Luo, M. Odor information processing by the olfactory bulb analyzed in gene-targeted mice. *Neuron* **65**, 912–926 (2010).
24. Cang, J. & Isaacson, J.S. *In vivo* whole-cell recording of odor-evoked synaptic transmission in the rat olfactory bulb. *J. Neurosci.* **23**, 4108–4116 (2003).
25. Isaacson, J.S. & Strowbridge, B.W. Olfactory reciprocal synapses: dendritic signaling in the CNS. *Neuron* **20**, 749–761 (1998).
26. Dietz, S.B. & Murthy, V.N. Contrasting short-term plasticity at two sides of the mitral-granule reciprocal synapse in the mammalian olfactory bulb. *J. Physiol. (Lond.)* **569**, 475–488 (2005).
27. Rinberg, D., Koulakov, A. & Gelperin, A. Sparse odor coding in awake behaving mice. *J. Neurosci.* **26**, 8857–8865 (2006).
28. Gheusi, G. *et al.* Importance of newly generated neurons in the adult olfactory bulb for odor discrimination. *Proc. Natl. Acad. Sci. USA* **97**, 1823–1828 (2000).
29. Imayoshi, I. *et al.* Roles of continuous neurogenesis in the structural and functional integrity of the adult forebrain. *Nat. Neurosci.* **11**, 1153–1161 (2008).
30. Linster, C. *et al.* Perceptual correlates of neural representations evoked by odorant enantiomers. *J. Neurosci.* **21**, 9837–9843 (2001).
31. Dhawale, A.K., Hagiwara, A., Bhalla, U.S., Murthy, V.N. & Albeanu, D.F. Non-redundant odor coding by sister mitral cells revealed by light addressable glomeruli in the mouse. *Nat. Neurosci.* **13**, 1404–1412 (2010).
32. Stopfer, M., Bhagavan, S., Smith, B.H. & Laurent, G. Impaired odor discrimination on desynchronization of odor-encoding neural assemblies. *Nature* **390**, 70–74 (1997).
33. Mwilaria, E.K., Ghatak, C. & Daly, K.C. Disruption of $GABA_A$ in the insect antennal lobe generally increases odor detection and discrimination thresholds. *Chem. Senses* **33**, 267–281 (2008).
34. Kay, L.M. & Stopfer, M. Information processing in the olfactory systems of insects and vertebrates. *Semin. Cell Dev. Biol.* **17**, 433–442 (2006).
35. Doucette, W. & Restrepo, D. Profound context-dependent plasticity of mitral cell responses in olfactory bulb. *PLoS Biol.* **6**, e258 (2008).
36. Doucette, W. *et al.* Associative cortex features in the first olfactory brain relay station. *Neuron* **69**, 1176–1187 (2011).
37. Chapuis, J. & Wilson, D.A. Bidirectional plasticity of cortical pattern recognition and behavioral sensory acuity. *Nat. Neurosci.* **15**, 155–161 (2012).
38. Uchida, N. & Mainen, Z.F. Speed and accuracy of olfactory discrimination in the rat. *Nat. Neurosci.* **6**, 1224–1229 (2003).
39. Rinberg, D., Koulakov, A. & Gelperin, A. Speed-accuracy tradeoff in olfaction. *Neuron* **51**, 351–358 (2006).
40. Nissant, A., Bardy, C., Katagiri, H., Murray, K. & Lledo, P.M. Adult neurogenesis promotes synaptic plasticity in the olfactory bulb. *Nat. Neurosci.* **12**, 728–730 (2009).
41. Mandairon, N. & Linster, C. Odor perception and olfactory bulb plasticity in adult mammals. *J. Neurophysiol.* **101**, 2204–2209 (2009).
42. Laurent, G. Olfactory network dynamics and the coding of multidimensional signals. *Nat. Rev. Neurosci.* **3**, 884–895 (2002).
43. Franks, K.M. & Isaacson, J.S. Strong single-fiber sensory inputs to olfactory cortex: implications for olfactory coding. *Neuron* **49**, 357–363 (2006).
44. Mouret, A. *et al.* Learning and survival of newly generated neurons: when time matters. *J. Neurosci.* **28**, 11511–11516 (2008).
45. Wilson, D.A. & Stevenson, R.J. Olfactory perceptual learning: the critical role of memory in odor discrimination. *Neurosci. Biobehav. Rev.* **27**, 307–328 (2003).
46. Mandairon, N., Stack, C., Kiselycznyk, C. & Linster, C. Broad activation of the olfactory bulb produces long-lasting changes in odor perception. *Proc. Natl. Acad. Sci. USA* **103**, 13543–13548 (2006).
47. Koulakov, A.A. & Rinberg, D. Sparse incomplete representations: a potential role of olfactory granule cells. *Neuron* **72**, 124–136 (2011).
48. Sahay, A., Wilson, D.A. & Hen, R. Pattern separation: a common function for new neurons in hippocampus and olfactory bulb. *Neuron* **70**, 582–588 (2011).

ONLINE METHODS

Animals. Adult (>2 months old, $n = 85$) male C57BL/6J mice were used in this study. Mice were housed under a 12-h light/dark cycle, with dry food and water available *ad libitum* except during behavioral experiments. All procedures were consistent with the European Communities Council Directive of 24 November 1986 (86/609/EEC) and the European Union guidelines, and were reviewed and approved by the Animal Welfare Committee of the Institut Pasteur.

Lentiviral vectors. A replication-deficient lentiviral vector based on the HIV virus was used to express a ChR2-YFP fusion construct driven by a synapsin 1 (*Syn1*) promoter using plasmids generously provided by K. Deisseroth (Stanford University, ChR2(H134R)-YFP for behavior and *in vitro and in vivo* electrophysiology experiments, and ChR2(E134T-H134R)-YFP for *in vivo* electrophysiology experiments). The concentration of lentiviral vector particles used for injection was 12 ng of viral antigen per µl assayed by ELISA (~10^{10} transduction units per ml).

Stereotaxic injection. Stereotaxic injections of lentiviral vector in adult mice were performed as previously described[49]. For lentiviral injections in postnatal mice, mouse pups at P6 were deeply anesthetized by immersion in ice for 8 min and positioned in a homemade cast. Small craniotomies were drilled above the injection sites with a needle. We performed bilateral virus injections (350 nl per site) as previously described into the RMS at +2.4 mm antero-posterior and ±0.6 mm medio-lateral from bregma, and −2.7 mm dorso-ventral from skull surface. Pups were placed back with their mother after recovery (30–60 min on a warm pad). After weaning (at P21), mice were segregated by gender.

Immunohistochemistry and imaging. We determined the density of YFP-positive cells in the different olfactory bulb layers from 1 to 35 weeks post-lentiviral vector injection. Free-floating coronal section and immunohistochemistry for YFP were carried out using chicken antibody to GFP (1:1,000, Upstate, 06-896) and Alexa-conjugated secondary antibody (1:500, Molecular Probes, A-11039) as previously described[50]. Stacks of optical slices (5 µm thick) were collected using an ApoTome microscope along the *z* axis of tissue sections from the whole olfactory bulb. The number cells expressing ChR2-YFP in the various zones was counted automatically with a dedicated computer program as previously described[44]. To correlate the density of YFP-positive cells in the GCL with behavioral performance, we killed all of the all mice in the ChR2 group at the end of the experiments.

Whole-cell patch-clamp recordings. Olfactory bulb slices, targeted whole-cell voltage-clamp recordings and histological studies after electrophysiological recordings were performed as previously described[22].

***In vitro* light stimulation.** We stimulated ChR2-positive neurons with a powerful LED array (Bridgelux) as previously described[22]. The maximum blue light (470 nm) intensity applied to the entire olfactory bulb slice was around 8.4 mW mm^{-2}. We varied the dose of light applied to the slices by changing the intensity of the LED. We delivered 5 or 20 consecutive pulses at 10 or 40 Hz, respectively, and repeated several sweeps at 5-s intervals. Fast-rising artifact-like responses to the onset and offset of the light were removed[22].

***In vivo* light stimulation.** Animals injected with lentiviral particles 8–10 weeks before were chronically implanted with a miniature LED (Osram, LED CMS 4.6W blue) as previously described[49]. The timing and intensity of the LED was controlled with a custom-built current-source circuit. For behavioral experiments, this device was synchronized to the olfactometer. All LEDs were tested before implantation and after termination of the experiments.

***In vivo* activation of ChR2-YFP–positive cells.** ChR2-YFP and c-Fos double staining was performed on olfactory bulb sections from animals previously injected with lentiviral vectors (5 months post-injection) and implanted with the miniature LED. Mice were divided in two groups: the light stimulated group that received three light-pulse trains of 90 s at 40 Hz every 2 min (5-ms pulses) and the no stimulated group that were manipulated identically, but not light stimulation were applied. For these experiments light intensity was slightly reduced to avoid overheating of the small LED. The mice were killed 1 h after stimuli delivery and the brains were processed for immnuhistochemistry as described previously. Incubation with both rabbit antibody to c-Fos (1:1,000, Santa Cruz, sc-52) and chicken antibody to GFP (1:1,000, Upstate) was performed in phosphate-buffered saline containing 0.2% Triton X-100 (vol/vol), 4% bovine serum albumin (wt/vol), 2% fetal calf serum (vol/vol, 4 °C for 2 d). The numbers of ChR2-YFP–positive, c-Fos–positive and double-stained cells were counted as previously described.

Behavioral apparatus. Mice were trained using custom-built computer-controlled eight-channel olfactometers as described previously[44] (http://www.olfacto-meter.com/). Odors were generated by passing a 140 cm^3 min^{-1} stream of air over the surface of diluted odorants in disposable 50-ml centrifuge tubes. The odorant vapor was mixed with 3,200 cm^3 min^{-1} clean air before its introduction into the sampling port. Thus, the odor concentration delivered was 4.3% that of the head space above the liquid odorant.

Odorants. Odorants (Sigma-Aldrich) were diluted with odorless mineral oil to the desired concentration, and 10 ml of solution was used as the odorant source. The liquid odorant was refreshed daily. The pairs of odorants and the dilutions used in all the experiments were divided into easy tasks (Easy 1, 1% anisole versus 1% cineole; Easy 2, 0.1% hexanol versus 0.1% octanal, first pair used in the training session in all experiments) and difficult tasks (Difficult 1, 1% (+)-carvone versus 1% (−)-carvone; Difficult 2, 0.1% (+)-limonene versus 0.1% (−)-limonene; Difficult 3, 1% (+)-terpinene versus 1% (−)- terpinene; Difficult 4, 0.6% of butanol + 0.4% pentanol versus 0.4% of butanol + 0.6% pentanol; Difficult 5, 0.6% of ethyl-butyrate + 0.4% amyl-acetate versus 0.4% of ethyl-butyrate + 0.6% amyl-acetate).

Pre-training procedures. Partially water-deprived mice (80–85% of their body weight) were trained using a go/no-go procedure. First, standard operant conditioning methods were used to train mice to insert their snouts into the odor sampling port and to respond by retracting the head and licking the water port (located on the left of odor sampling port) in the presence of an odorant. The mice initiated each trial by breaking the light beam positioned across the odor sampling port. This led to the opening of an odor valve and a diversion valve directing all airflow away from the sampling tube. This resulted in the odorant vapor being combined with the main air stream and the diversion of the main air stream to an exhaust path. The diversion valve relaxed 1 s later and the odor stimulus was presented to the odor sampling port. The stimulus valve relaxed 2 s later (maximum odor stimulus duration), terminating delivery of the odor. Reward delivery depended on the mouse licking the water delivery tube (maximum response criterion, 2 s). Trials in which the mouse did not keep its snout in the odor sampling port for at least 0.1 s after odor onset were aborted and counted as short sample trials. A 3-µl water reward was delivered if the mouse satisfied the response criterion. The mouse had then to retract its head (the beam was resealed) and wait at least 5 s (intertrial interval) before initiating a new trial. All mice underwent five pre-training sessions.

Training procedures. The trial procedures were identical with those used in the initial pre-training sessions. Mice were trained to respond to the presence of an odor (positive stimulus) by licking the water port and to refrain from responding to the presence of another odor (negative stimulus). In each trial, a single stimulus (positive or negative) was presented. If the response criterion was met in positive stimulus trials, a droplet of water (3 µl) was given as a reward and the trial was scored as a hit. Failing to lick in negative stimulus trial was scored as a correct rejection. Positive and negative stimulus trials were presented in a modified random order (each block contained equal numbers of positive and negative stimulus trials, do not presented more than three times consecutively). The percentage of correct responses was determined for each block of 20 trials ((hits + correct rejections)/20 × 100). Scores ≥85% implied that mice had correctly learned to assign the reward value of the positive stimulus and the non-reward value of the negative stimulus. All trained mice underwent ten blocks per day. The number of blocks to reach the criterion level was counted as the number of blocks employed to reach the first block at 85% of corrected responses. To provide photostimulation, the LED was connected to the control system before the mouse was placed in the olfactometer. Light onset was synchronized with the relaxation of the diversion valve that produces odor stimulus presentation to the odor sampling (paired protocol) or delay of 500 ms (delayed protocol) for both positive stimulus and negative stimulus. The duration of light stimulation was always 500 ms at both 40 Hz (20 pulses of 5 ms) or 10 Hz (five pulses of 5 ms). The absolute light intensity was calibrated before each experiment (**Supplementary Fig. 2**).

Olfactory discrimination learning sessions. Mice were first trained to discriminate an easy odor pair to become familiar with the go/no-go task without light stimulation (accuracy of 90% after 500 trials). Thereafter, animals were trained to discriminate an easy pair while receiving light stimulation in each single trial using a 40-Hz paired protocol. Subsequently, each mouse learned to discriminate at least two different difficult pairs, using different light stimulation protocols. Subsequently, odorant detection threshold or acuity was analyzed. For detection threshold, mice were trained to detect successively lower concentrations of (+)-carvone diluted in mineral oil (one concentration per day for ten blocks). In each session, (+)-carvone served as the positive stimulus and mineral oil served as the negative stimulus. The concentrations of (+)-carvone used in these tasks were 1, 0.1, 0.01, 0.001 and 0.0001%. Finally, to evaluate discrimination acuity, animals were trained to discriminate mixtures with increasing complexity. Mice were first trained to distinguish between 1% (+)-carvone and 1% (−)-carvone. Then, they were learned to discriminate between mixtures of these odors. The first mixture pair was composed of 80% of (+)-carvone and 20% of (−)-carvone for positive stimulus versus 80% of (−)-carvone and 20% of (+)-carvone for negative stimulus. In each successive task, the same procedures were followed, but the concentration of both enantiomers in the mixture was sequentially equalized in separate sessions (one per day) to (+)-carvone/(−)-carvone (%): 60/40, 55/45 and 52/48 for positive stimulus versus 40/60, 45/55 and 48/52 for negative stimulus. Each mixture was given for ten blocks each day. For both detection threshold and discrimination acuity experiments, light stimulation was synchronized with both odor stimuli at 40 Hz (paired protocol).

Each mouse was tested on one particular task per day. All behavioral data were exported and stored in a MySQL engine database. Behavioral analyses were performed with Data Dock, a custom-built software written in the php language and connected to the database. Accuracy was expressed as mean of percentage of correct responses for five training blocks, except for **Figures 2c**,**e** and **3f**,**g** and **Supplementary Figures 5a** and **6**.

Discrimination time. The odor sampling time (discrimination time) is the latency from odor onset to withdrawal of nose from odor port. For more details, see **Supplementary Figure 3**.

Olfactory memory. We determined the time over which mice were able to discriminate between two odorants and remember their value (rewarded or non-rewarded). The mice were trained using easy or difficult tasks and were exposed to the same task again 10, 30 or 50 d later. For the memory tests, the procedures were identical with those previously described for training, except for the length of the session (only two blocks) and for the absence of water reward.

***In vivo* electrophysiological recordings.** For head fixation, anesthetized mice were first implanted with a L-shaped metal bar fixed with dental cement to the caudal part of the skull. After recovery (5 d), implanted animals were progressively habituated to stay quiet while head-restrained (7 d). The mouse was anesthetized 1 d before recording and the bone covering the left or right bulb was thinned using a microdrill to allow the opening of a small hole on the following day. Mitral cell spiking activity was recorded in the ventral part of the bulb using 3 MΩ tungsten electrodes (FHC) glue parallel to an optic fiber to ensure local illumination of above GCL nearby the recorded cell. The distance between the tips of the fiber and electrodes was 400–500 µm. The optic fiber (multimode, 0.22-mm diameter, NA = 0.5, Doric Lenses) was coupled to a miniature blue LED (470 nm, Doric Lenses) controlled by a custom-built DC driver (output light intensity 2.5–3 mW). The estimated number N of light-stimulated adult-born granule cells in the cone of blue light of the optic fiber was calculated by

$$N = \frac{D\pi h}{3}({r_{max}}^2 + r_{max}r_{fib} + {r_{fib}}^2) \text{ and } r_{max} = r_{fib} + \tan(\sin^{-1}\left(\frac{NA}{n_{gm}}\right))h$$

with D being the volumic density of ChR2-positive neurons (~12,500 cells per mm^3), h being the distance from the optic fiber tip in the GCL to the electrode tip in the mitral cell layer (MCL, 400–500 µm), r_{fib} being the radius of the optic fiber (0.11 mm), NA being its numerical aperture (0.5), n_{gm} being the refractive index of the gray matter (1.36), and r_{max} being the radius of illumination at distance h.

Both local field potentials and spiking activity were pre-amplified (unitary gain headstage, WPI), amplified (×10,000, WPI), filtered (1–300 Hz for LFP, 300–10,000 Hz for spikes) and digitized at 25 kHz (A/D interface, CED). The identity of mitral cell was established on the basis of several criteria: stereotaxic coordinates of the ventral mitral cell layer (MCL; AP: 5.1, ML: 0.9, DV: -2.7), decrease in the gamma oscillation amplitude in the MCL compared with the local field potential recorded in the GCL or external plexiform layer, where the current source/sink of gamma oscillation are localized[51], increase in background spiking activity in a narrow band of 100–150 µm corresponding to MCL, and typical spontaneous activity patterns time-locked to the respiration rhythm, although cell rhythmicity is less obvious in the awake state than in the anesthetized state[27]. Spike detection, spike sorting, spike waveform analysis and PSTHs were performed with Spike2 software (CED). For single-unit validation, all sorted cells displayed less than 1% of their interspike intervals below a 3.5-ms refractory period. For light stimulation during spontaneous activity, each 1-s train stimulus (10 Hz or 40 Hz) were presented every 10 s. For odor presentation, we used a custom-built flow-dilution olfactometer controlled by the CED interface with a 5 l min^{-1} flow presented 2 cm from the mouse nose. Pure monomolecular odorants (Sigma-Aldrich) were diluted in mineral oil (10%) in odorless plastic vial. Saturated odor vapor was further diluted with humidified clean air (1:10) by means of computer-controlled solenoids pinch valves. Odors were presented for 3 s every 60 s (to reduce sensory adaptation) over 10–30 repetitions for each experimental condition (10 Hz, 40 Hz and no light). Each odor presentation was preceded and followed by 10 s of clean air. The odorants used in the final data set were butyraldehyde (n = 3 cells), valeraldehyde (n = 2), heptanal (n = 3), octanal (n = 1), ethylbutyrate (n = 5), buthylbutyrate (n = 1), peppermint (n = 3), anisol (n = 1), cineole (n = 1), β-ionone (n = 1) and (−)-limonene (n = 1). Spontaneous firing activity was measured using PSTHs during the 1-s light stimulation and compared with the 1-s period preceding and following stimulation. Odor-evoked activity was calculated as a z score by $(FR_L - FR_B) / (FR_L + FR_B)$, where FR_L is the mean firing rate during light stimulation coupled to odor presentation and FR_B is the mean firing rate during odor presentation without light.

Statistical analyses. Statistical analyses were performed with Prism and Statistica softwares. All data sets were described using the mean. Differences were considered significant for $P < 0.05$.

49. Lepousez, G., Alonso, M., Wagner, S., Gallarda, B.W. & Lledo, P.-M. Selective viral transduction of adult-born olfactory neurons for chronic *in vivo* optogenetic stimulation. *J. Vis. Exp.* published online, doi:10.3791/3380 (28 December 2011).
50. Alonso, M. *et al.* Turning astrocytes from the rostral migratory stream into neurons: a role for the olfactory sensory organ. *J. Neurosci.* **28**, 11089–11102 (2008).
51. Neville, K.R. & Haberly, L.B. Beta and gamma oscillations in the olfactory system of the urethane-anesthetized rat. *J. Neurophysiol.* **90**, 3921–3930 (2003).